Chapter 6
Computer-Assisted Treatment Planning Approaches for SBRT

Taiki Magome

Abstract This chapter describes computer-assisted treatment planning approaches for stereotactic body radiation therapy (SBRT), focusing especially on beam angle optimization and similar-case-based treatment planning. The determination of appropriate treatment plans for SBRT is a substantial and demanding task for inexperienced treatment planners. A computer-aided treatment planning system for SBRT could help treatment planners by capitalizing on the knowledge and skills that are stored in radiotherapy treatment planning databases. First, the chapter describes a computer-aided method of determining beam arrangements based on similar cases in a radiotherapy treatment planning database. Second, the chapter discusses a similar-case-based optimization method for beam arrangements that was designed to assist treatment planners. The methods introduced herein could be employed as computer-aided tools that assist treatment planners. The quality of radiotherapy could thus be normalized across treatment planners with different levels of experience in SBRT.

Keywords Treatment planning • Similar case • Knowledge based • Computer aided • Stereotactic body radiation therapy

6.1 Introduction

Stereotactic body radiation therapy (SBRT) can be used to deliver highly conformal doses to tumors while minimizing doses to surrounding organs at risk (OARs) and normal tissues with steep dose gradients (Nagata et al. 2005, Takayama et al. 2005; Timmerman et al. 2006a, 2007; Glide-Hurst and Chetty 2014). In general, hypofractionated regimens (10–20 Gy in five or fewer fractions) have been used. Numerous phase I/II studies of early-stage lung and liver cancers have shown high local control rates and good tolerability (Nagata et al. 2005, 2011; Timmerman et al. 2006b, 2010; Onishi et al. 2011; Taremi et al. 2012; Shioyama et al. 2013).

T. Magome (✉)
Department of Radiological Sciences, Faculty of Health Sciences, Komazawa University, 1-23-1, Komazawa, Setagaya-ku, Tokyo 154-8525, Japan
e-mail: magome@komazawa-u.ac.jp

H. Arimura (ed.), *Image-Based Computer-Assisted Radiation Therapy*,
DOI 10.1007/978-981-10-2945-5_6

Recently, this technique has made substantial progress with intensity-modulated radiation therapy (IMRT), volumetric modulated arc therapy (VMAT), and flattening filter-free (FFF) beams (Videtic et al. 2010; Holt et al. 2011; Zhang et al. 2011; Takahashi et al. 2013; Hrbacek et al. 2014; Nakagawa et al. 2014; Yamashita et al. 2014a).

Radiotherapy treatment planning (RTP), which is one of the most important procedures for SBRT, is determined by treatment planners in a time-consuming iterative manner. In particular, it is essential to determine an appropriate beam arrangement, which generally consists of a large number of coplanar and noncoplanar static beams or rotational beams (Takayama et al. 2005; Liu et al. 2006; Lim et al. 2010).

In general, the choice of an appropriate beam arrangement for lung SBRT has varied across institutions, depending on their individual circumstances. Regarding the number of beams, Takayama et al. (2005) reported routine use of five to ten beams with coplanar and noncoplanar directions in order to deliver homogeneous target dose distributions during lung SBRT, while avoiding high doses to normal tissues. Liu et al. (2006) found that the optimal number of beams for lung SBRT was 13–15 with coplanar and noncoplanar directions. A large number of beams increase the required treatment time, which should be as short as possible to reduce intra-fractional patient motion. Moreover, the available beam direction space is restricted by the size of the gantry and the immobilizer. The beam arrangement plans are not limited to the beam directions; planning also includes nominal beam energies, collimator angles, beam weights, and other parameters.

One of the most difficult problems in RTP is the patient-specific trade-off between the benefit of irradiating the tumor and the risk to surrounding normal tissues. Therefore, treatment planners should select a plan that is most suitable for the individual patient who is in their care. In the rest of this chapter, several methods of overcoming the abovementioned problems are discussed.

6.2 Target and Organ Determination in SBRT

The majority of treatment planning procedures for SBRT are the same as those used for conventional treatment planning: (1) contouring of a target and OARs, (2) determination of the beam arrangements, and (3) optimization of the dose distribution (via a trial-and-error approach or inverse planning, such as in IMRT and VMAT). The four-dimensional motions of the target and OARs should be considered in SBRT. Report 62 of the International Commission on Radiation Units & Measurements (ICRU 1999) introduced the concept of the internal target volume (ITV), in which the internal margin due to physiological motion (e.g., respiration) is added to clinical target volume (CTV). The ITV can be created individually according to the internal respiratory motion of the patient, which can be measured with an X-ray simulator or four-dimensional computed tomography (4DCT) (Underberg et al. 2004; Rietzel et al. 2005; Yamashita et al. 2014b). When 4DCT is used for this

purpose, the motions of the target and organ are visualized in different phases of the respiratory cycle. CTVs can be delineated on all 4DCT phases, and a union can be defined as the ITV.

6.3 Beam Angle Optimization

Many researchers have investigated automated methods for beam angle optimization (BAO) (Rowbottom et al. 1999; Pugachev and Xing 2002; Djajaputra et al. 2003; Gaede et al. 2004; Wang et al. 2004; Meyer et al. 2005; de Pooter et al. 2006, 2008; Liu et al. 2006; Aleman et al. 2008; Potrebko et al. 2008; Li and Lei 2010; Vaitheeswaran et al. 2010; Breedveld et al. 2012; Bertsimas et al. 2013). Rowbottom et al. (1999) suggested a method in which the coplanar beam orientation was determined using an artificial neural network. Li et al. (Li and Lei 2010) developed a DNA-based genetic algorithm to solve the BAO problem in coplanar directions for IMRT planning. De Pooter et al. (2006, 2008) investigated an optimization method for noncoplanar beams based on the cycle algorithm for SBRT of liver tumors. Meyer et al. (2005) developed an automated method for the selection of noncoplanar beams by using a cost function based on radiation absorption in normal tissue and OARs for three-dimensional conformal radiotherapy. The majority of the abovementioned methods maximize or minimize a cost function, which is often defined without information on the dose distribution in order to reduce computational costs. Treatment planning time could be reduced by using these BAO algorithms, as compared with trial-and-error approaches.

6.4 Similar-Case-Based Treatment Planning

In the field of diagnostic radiology, the presentation of similar cases as a diagnostic aid has been suggested when making diagnoses based on chest images (Aisen et al. 2003), lung computed tomography images (Kumazawa et al. 2008), and mammography images (Kumazawa et al. 2008, Muramatsu et al. 2005, 2009, 2010). These studies have indicated that it is feasible to use similar cases as a diagnostic aid. To date, the usefulness of similar cases in the field of radiation oncology has been shown in several studies. Commowick and Malandain (2007) used a similar image in a database for the segmentation of critical structures. Chanyavanich et al. (2011) developed new prostate IMRT plans based on similar cases. Mishra et al. (2011) investigated the case-based reasoning approach to determine the most appropriate dose plans for prostate cancer patients. Schlaefer and Dieterich (2011) showed the feasibility of case-based beam generation for robotic radiosurgery. Therefore, the clinically usable beam arrangements for SBRT might also be determinable based on past similar cases.

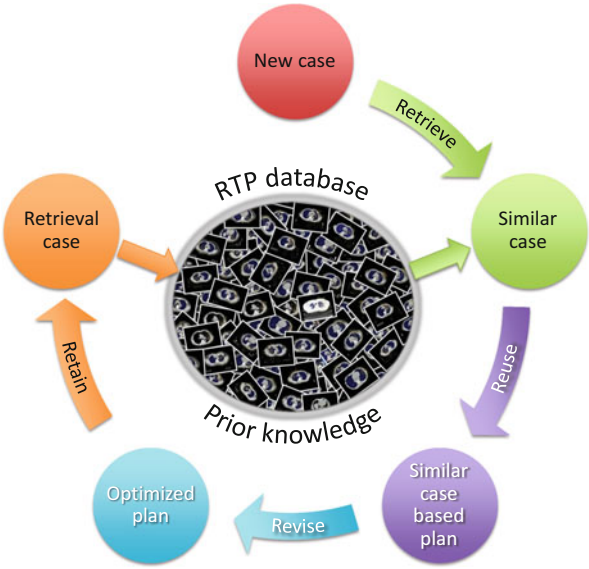

Fig. 6.1 Conceptual scheme of similar-case-based radiotherapy treatment planning

RTP is a time-consuming task, especially for less experienced treatment planners. Treatment planning skills are developed by repeated planning experiences in clinical practice, often under the guidance of experienced planners or appropriate textbooks. As they gain experience, treatment planners should memorize many planning patterns and construct an evolving "database" in their memory, which can then be searched for past cases that are similar to the case under consideration. Therefore, a similar-case-based treatment planning tool (Fig. 6.1) may reduce both the workload for treatment planners and the inter-planner variability of treatment plans. Moreover, the similar-case-based approach to RTP could be adjusted to the specific circumstances and contexts of different institutions by replacing the RTP database.

6.5 Similar-Case-Based Beam Angle Optimization

The accuracy and efficiency of beam arrangement determinations could potentially be improved by combining similar-case-based treatment planning and BAO algorithms (Magome et al. 2013a, b). Figure 6.2 shows the overall scheme of the similar-case-based beam angle optimization method, which consisted of three main steps. First, cases that were similar to an objective case were automatically selected from the RTP database based on geometrical features related to structures, such as the location, size, and shape of the target and OARs. Second, the initial beam arrangements of the objective case were determined by registering similar cases to the objective case, using a linear registration technique (Burger and Burge

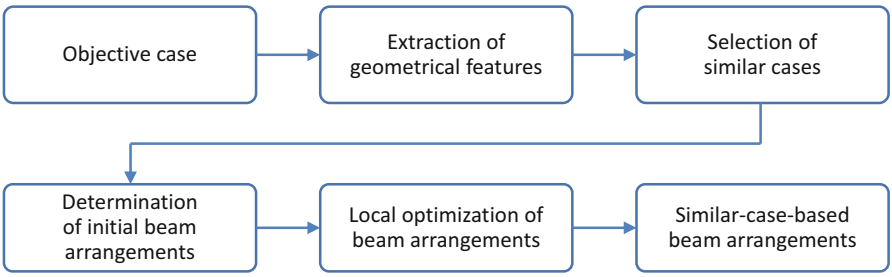

Fig. 6.2 Overall scheme of similar-case-based beam angle optimization

2007). Finally, the beam directions of the objective case were locally optimized based on the cost function, which took the radiation absorption in normal tissues and OARs into account.

6.5.1 Feature Extraction for Searching Similar Cases

It is very important to consider the exact meaning of "similarity" in the radiation oncology field. "Similarity" could be defined in many different ways, for example, based on the similarity of the tumor type (histological type or staging), the patient (gender, age, height, weight, etc.), or other characteristics. However, similar cases should be defined from the viewpoint of treatment planning because they are intended to be useful for the treatment planner. It should be assumed that the geometrical similarity with respect to tumor and OAR among clinical cases may be a key in the similar-case-based treatment planning. Therefore, four types of features (comprising 10 features in total) were defined for lung SBRT: the planning target volume (PTV) shape, the PTV size, the lung dimensions, and the geometrical relationship between the PTV and the spinal cord (Fig. 6.3), as assessed using the DICOM-RT structure set (Magome et al. 2013a).

The ten defined geometrical features were described as follows: PTV centroid in left-right (*LR*), anterior-posterior (*AP*), and superior-inferior (*SI)* directions; effective diameter of the PTV; sphericity of the PTV; lung dimension in *LR*, *AP*, and SI directions; distance between the PTV and the spinal cord in the isocenter plane; and angle from the spinal cord to the PTV in the isocenter plane. The PTV centroid was determined by registering the lung structure image of each case in the RTP database with that of a reference case, using a linear registration technique (Burger and Burge 2007). The effective diameter was defined as the diameter of a sphere with the same volume as the PTV. The sphericity was defined as the roundness of the PTV without directional dependence, and given by the ratio of the number of logical AND voxels between the PTV and its equivalent sphere with the same centroid and volume as the PTV to the number of PTV voxels. The lung dimensions were defined as the three side lengths of the circumscribed parallelepiped of the

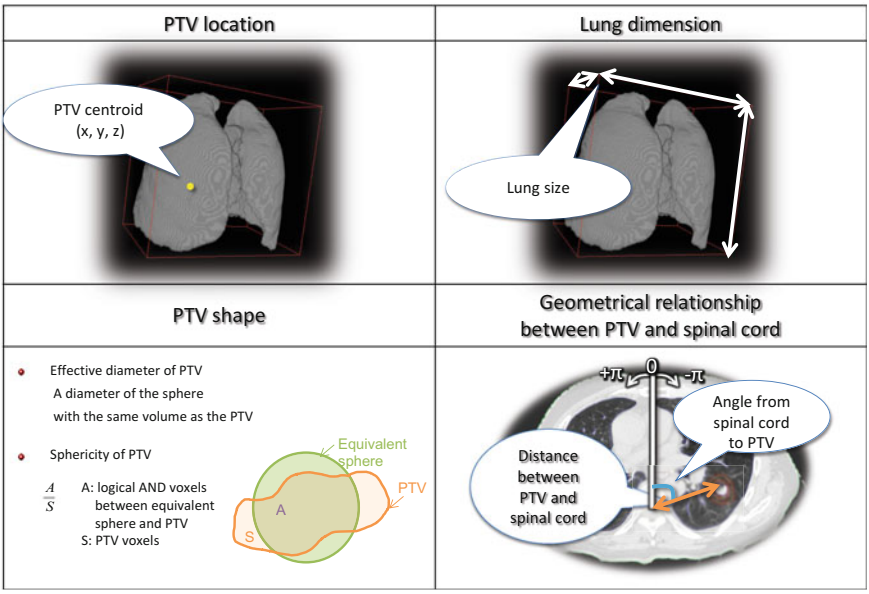

Fig. 6.3 Geometrical features, which were used to search for similar cases in a lung SBRT database (Magome et al. 2013a)

lung regions in the *LR*, *AP*, and *SI* directions. The distance between the PTV and spinal cord was measured between the centroid of the PTV and that of the spinal cord in the isocenter plane. The angle from the spinal cord to the PTV was defined in the two-dimensional coordinate system with the origin at the centroid of the spinal cord in the isocenter plane, and ranged from $-\pi$ (clockwise) to π (counter-clockwise) for a baseline of the posterior-anterior direction. Although only the PTV centroid was determined in a fixed reference coordinate system by registering the lung regions of each case in the RTP database with those of a reference case, the other features were calculated with respect to each of their original coordinate systems. The calculations were performed in this way in order to consider both the relative similarity of the tumor in the lung regions and absolute similarities, such as of the lung dimensions and spinal cord position.

6.5.2 *Selection of Similar Planning Cases Using Geometrical Features*

The RTP database was searched for the cases that resembled the objective case by considering the weighted Euclidean distances between the geometrical feature vector of the objective case and the geometrical feature vectors of all other cases in the RTP database (Fig. 6.4). The weighted Euclidean distance was thus regarded

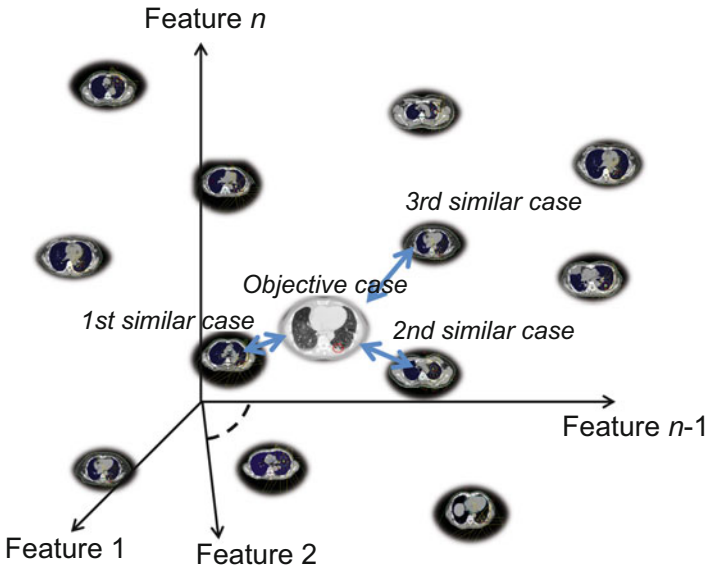

Fig. 6.4 Conceptual illustration of an objective case and similar cases in a n-dimensional feature space. Most similar case was defined as the case that was closest to the objective case in the feature space, as measured with a weighted Euclidean distance

as a similarity measure. The weighted Euclidean distance d_{image} was calculated using the following equation:

$$d_{\text{image}} = \sqrt{\sum_{i=1}^{G} w_i (A_i - B_i)^2}, \tag{6.1}$$

where G is the number of geometrical features, w_i is the weight of the i-th geometrical feature, A_i is the i-th geometrical feature for the objective case, and B_i is the i-th geometrical feature for another case in the RTP database. Note that each geometrical feature was normalized by subtraction of a mean of the feature and dividing it by the standard deviation of its value for all cases in the RTP database.

Weights were needed for the geometrical features in order to incorporate their relative importance from the viewpoint of treatment planning. Therefore, when applying the proposed method to their own databases, each institute should determine the appropriate weights for the geometrical features based on their own philosophy or policy of treatment planning. In our investigation, the weights for geometrical features were empirically set as follows: PTV centroid (three-dimension) = 0.3, effective diameter of PTV = 0.1, sphericity of PTV = 0.1, lung dimension (three-dimension) = 0.3, distance between PTV and spinal cord = 1.0, and angle from spinal cord to PTV = 1.0.

6.5.3 Determination of Initial Beam Arrangements Based on the Linear Registration Technique

In the second step, beam arrangements for the objective case were automatically determined (Magome et al. 2013a) based on the registration of similar cases with the objective case in terms of lung regions, using a linear registration technique (i.e., affine transformation) (Burger and Burge 2007). The beam arrangement of the similar case was modified to fit the objective case with respect to the lung regions.

First, a beam angle (i.e., a beam direction with a gantry angle θ and couch angle φ) was described as a point in a Cartesian coordinate system. As shown in Fig. 6.5, the beam direction with gantry angle θ and couch angle φ can be considered as a line in a spherical polar coordinate system, with the origin as the isocenter. An arbitrary point ($x_{\theta,\varphi}$, $y_{\theta,\varphi}$, $z_{\theta,\varphi}$) on the line is described in a Cartesian coordinate system as follows:

$$\begin{pmatrix} x_{\theta,\phi} \\ y_{\theta,\phi} \\ z_{\theta,\phi} \end{pmatrix} = \begin{pmatrix} x_{\mathrm{iso}} + r\sin\theta\cos\phi \\ y_{\mathrm{iso}} - r\cos\theta \\ z_{\mathrm{iso}} + r\sin\theta\sin\phi \end{pmatrix}. \tag{6.2}$$

where r is distance from the isocenter (x_{iso}, y_{iso}, z_{iso}). In this study, r has no meaning ($r = 1$ for simplicity) because the purpose of the analysis is registration of the beam angle.

Second, each beam point of the similar case in the Cartesian coordinate system was modified based on a linear registration technique (i.e., an affine transformation) (Burger and Burge 2007). Please note that the linear registration maps straight lines to straight lines, and thus the beam directions—which can be considered as points—are uniquely and automatically determined by the registration. The beam point ($x_{\theta,\varphi}$, $y_{\theta,\varphi}$, $z_{\theta,\varphi}$) was modified to the point ($x'_{\theta,\varphi}$, $y'_{\theta,\varphi}$, $z'_{\theta,\varphi}$) by using the affine transformation matrix to register the lung regions of each similar case with those of the objective case, as follows:

$$\begin{pmatrix} x'_{\theta,\phi} \\ y'_{\theta,\phi} \\ z'_{\theta,\phi} \\ 1 \end{pmatrix} = \begin{pmatrix} u_{11} & u_{12} & u_{13} & u_{14} \\ u_{21} & u_{22} & u_{23} & u_{24} \\ u_{31} & u_{32} & u_{33} & u_{34} \\ 0 & 0 & 0 & 1 \end{pmatrix} \begin{pmatrix} x_{\theta,\phi} \\ y_{\theta,\phi} \\ z_{\theta,\phi} \\ 1 \end{pmatrix}, \tag{6.3}$$

where $u_{11}\ldots u_{34}$ are the transformation parameters. The isocenter point (x_{iso}, y_{iso}, z_{iso}) was also modified to the point (x'_{iso}, y'_{iso}, z'_{iso}) in the same manner. The affine transformation can apply a linear combination of translation, scaling, rotation, and/or shear mapping. Further details can be found in the literature (Burger and Burge 2007). The vertices of a circumscribed parallelepiped of a lung (including the left and right lung regions) were automatically obtained as feature points to calculate the parameters of the affine transformation matrix. In this study, the

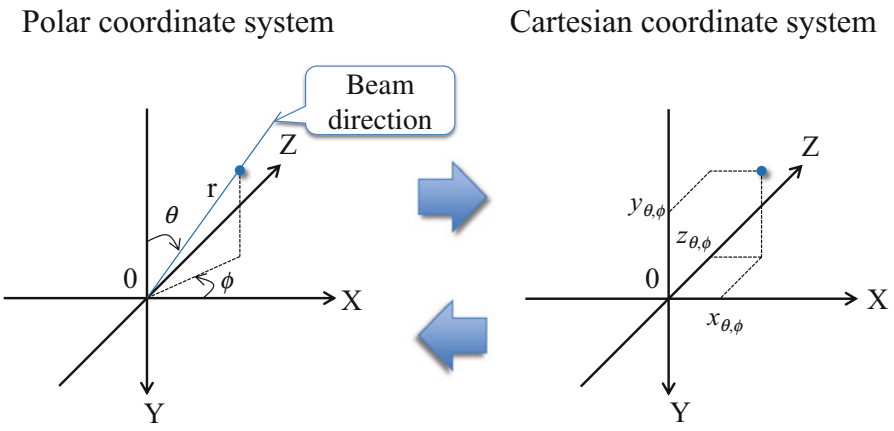

Fig. 6.5 Illustration of a beam direction with gantry angle θ and couch angle φ in a spherical polar coordinate system and a Cartesian coordinate system. Here, the origin indicates an isocenter and couch angle φ is defined with respect to the patient-fixed coordinate system

circumscribed parallelepiped was chosen to reduce the calculation time that was necessary to find the feature points of the lung.

Finally, the resulting direction vector ($x'_{\theta,\varphi} - x'_{\mathrm{iso}}$, $y'_{\theta,\varphi} - y'_{\mathrm{iso}}$, $z'_{\theta,\varphi} - z'_{\mathrm{iso}}$) in the Cartesian coordinate system was converted into the spherical polar coordinate system as gantry angle θ' and couch angle φ', as follows:

$$\theta' = \tan^{-1}\left(\frac{\sqrt{\left(x'_{\theta,\phi} - x'_{\mathrm{iso}}\right)^2 + \left(z'_{\theta,\phi} - z'_{\mathrm{iso}}\right)^2}}{-\left(y'_{\theta,\phi} - y'_{\mathrm{iso}}\right)}\right), \tag{6.4}$$

$$\phi' = \tan^{-1}\left(\frac{\left(z'_{\theta,\phi} - z'_{\mathrm{iso}}\right)}{\left(x'_{\theta,\phi} - x'_{\mathrm{iso}}\right)}\right). \tag{6.5}$$

6.5.4 *Local Optimization of Beam Arrangements*

The beam directions of the objective case were locally optimized based on the cost function, which took into account the radiation absorption in normal tissues and OARs (Magome et al. 2013b). Although Meyer et al. (2005) developed the cost function for a global optimization of beam arrangements, the cost function was used for the local optimization of each beam direction in this study. The cost function $C_{\theta,\varphi}$ of a beam with gantry angle θ and couch angle φ was defined as follows:

$$C_{\theta,\varphi} = C_{\theta,\varphi}(\mathrm{PTV}) + \sum_k w_k C_{\theta,\varphi}(\mathrm{OAR}_k), \tag{6.6}$$

where $C_{\theta,\varphi}(\mathrm{PTV})$ represents the dose absorption in normal tissue until the X-ray beams reach the PTV surface, $C_{\theta,\varphi}(\mathrm{OAR}_k)$ is a term for the irradiation of k-th OAR, and w_k is a weight for the k-th OAR. The first term $C_{\theta,\varphi}(\mathrm{PTV})$ was determined by the following equation:

$$C_{\theta,\varphi}(\mathrm{PTV}) = 1 - \exp\bigl(-\mu d_{\theta,\varphi}(\mathrm{PTV})\bigr), \tag{6.7}$$

where μ is a linear attenuation coefficient in water, and $d_{\theta,\varphi}(\mathrm{PTV})$ is the mean distance in centimeters from the body surface to the PTV surface. The second term for the k-th OAR $C_{\theta,\varphi}(\mathrm{OAR}_k)$ was defined as follows:

$$C_{\theta,\phi}(\mathrm{OAR}_k) = \lambda v_{\theta,\phi}(\mathrm{OAR}_k) + (1-\lambda)\exp\bigl(-\mu d_{\theta,\phi}(\mathrm{OAR}_k)\bigr), \tag{6.8}$$

where $v_{\theta,\varphi}(\mathrm{OAR}_k)$ is an irradiated fractional volume of the k-th OAR, $d_{\theta,\varphi}(\mathrm{OAR}_k)$ is the mean depth from the body surface to the k-th OAR surface, and λ is a parameter for controlling the relative significance of the first and second terms. The term $\exp(-\mu d_{\theta,\varphi}(\mathrm{OAR}_k))$ represents the number of incident photons in the k-th OAR. Figure 6.6 presents a conceptual illustration of the cost function.

Each beam direction was locally optimized in the range of $\pm\, p$ degrees at an interval of q degrees. The lung and spinal cord were incorporated as OARs in the cost function, and both weights (for the lung and the spinal cord) were set to 5.0. The parameters for the local optimization of the beam arrangement λ, p, and q, were set to 0.6, 4°, and 2°, respectively. Although the parameters for the local optimization of beam arrangements were set empirically based on the preferences of our institution, each institute could determine the appropriate parameters based on their own philosophy or policy of treatment planning, in resemblance with the geometrical feature weights. Each optimal beam direction was defined as the direction of the beam which had the lowest cost value among the beam directions of the local range.

6.5.5 *Evaluation of Beam Arrangements Using Planning Evaluation Indices*

The similar-case-based beam arrangements were evaluated by manually preparing plans based on both the beam arrangements and other planning parameters (such as nominal beam energies, collimator angles, and beam weight) derived from the treatment plans of similar cases in a radiation treatment planning system. The following 11 planning evaluation indices were used for validation.

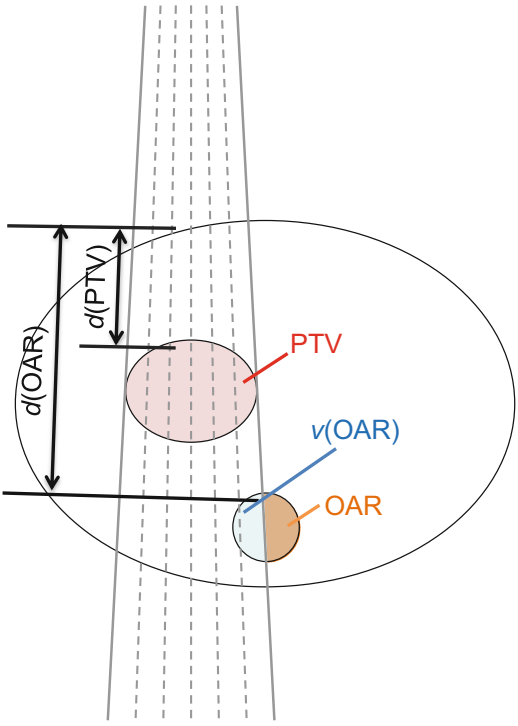

Fig. 6.6 Conceptual diagram of the cost function for local optimization of beam angles

The planning evaluation indices for the PTVs calculated in this study were the D95, homogeneity index (HI), conformity index (CI), and tumor control probability (TCP). The D95 was defined as the minimum dose in the PTV that encompassed at least 95 % of the PTV. The HI was calculated as the ratio of the maximum dose to the minimum dose in the PTV. The CI was the ratio of the treated volume to the PTV. The treated volume was defined as the tissue volume that was receiving the minimum PTV dose. The TCP was estimated based on a linear-quadratic (LQ) model according to a Poisson distribution by considering the radiosensitivity variation and nonuniform dose distribution (Sanchez-Nieto and Nahum 1999, 2000). The TCP was averaged over a population with variability in radiosensitivity, which was simulated as a Gaussian distribution of α_k values with mean $\overline{\alpha}$ and standard deviation σ_α in K groups of patients (Webb and Nahum 1993; Kanai et al. 2006). Specifically, TCP was given by

$$\mathrm{TCP} = \sum_{k=1}^{K} \left(\frac{1}{\sqrt{2\pi}\sigma_\alpha} \right) \exp\left\{ -\frac{(\alpha_k - \overline{\alpha})^2}{2\sigma_\alpha^2} \right\} \times \prod_{l=1}^{L} \exp\left[-\rho_c v_l \cdot \exp\left\{ -\alpha_k D_l \left(1 + \frac{d_l}{\alpha_k/\beta_k} \right) \right\} \right], \tag{6.9}$$

where ρ_c is the number of initial clonogenic cells per volume cm^3, L is the number of dose bins of the differential dose-volume histogram (DVH) in the PTV, v_l is the volume (cm^3) irradiated by a dose d_l (Gy) per fraction in the PTV, and D_l is the total dose (Gy) at v_l. The α_k ranged $\alpha_k \pm \gamma\sigma_\alpha$, and increased in certain intervals divided by K. The parameters for the TCP calculation were obtained from Kanai et al.'s (2006) study of patients with lung cancers.

The planning evaluation indices for normal tissues (i.e., the lung and spinal cord) were calculated as described below. For the lung volume, which was defined as the total lung volume minus the PTV, a $V5$, $V10$, $V20$, and mean dose were calculated. Each Vk was defined as the percentage of the total lung minus PTV receiving $\geq k$ Gy. The maximum dose for the spinal cord was also calculated. Moreover, the normal tissue complication probability (NTCP) values for the lung and spinal cord were calculated using the Lyman-Kutcher-Burman model (Lyman 1985; Kutcher and Burman 1989; Burman et al. 1991). For the calculation of the NTCP, the dose scale of a DVH was rescaled as a linear-quadratic equivalent dose (LQED) for 2 Gy fractions, as follows:

$$\mathrm{LQED}_s = D_s \frac{\alpha/\beta + d_s}{\alpha/\beta + 2}, \tag{6.10}$$

where D_s is the total dose (Gy), α/β is a parameter for a linear-quadratic model (Wheldon et al. 1998; Thames et al. 1990), and d_s is the dose per fraction (Gy) at D_s in the differential DVH. Then, the NTCP was calculated as

$$\mathrm{NTCP} = \frac{1}{\sqrt{2\pi}} \int_{-\infty}^{t} \exp\left(-\frac{x^2}{2} \right) dx = \frac{1}{2} \left\{ 1 + \mathrm{erf}\left(\frac{t}{\sqrt{2}} \right) \right\}, \tag{6.11}$$

$$t = \frac{\mathrm{LQED}_{\max} - TD_{50}(v)}{mTD_{50}(v)}, \tag{6.12}$$

$$v = \frac{v_{\mathrm{eff}}}{v_{\mathrm{ref}}}, \tag{6.13}$$

$$v_{\mathrm{eff}} = \sum_{s=1}^{S} \left(\frac{\mathrm{LQED}_s}{\mathrm{LQED}_{\max}} \right)^{1/n} v_s, \tag{6.14}$$

$$TD_{50}(v) = TD_{50}(v_{\mathrm{ref}}) \cdot v^{-n}, \tag{6.15}$$

where erf(·) is an error function, $TD_{50}(v)$ and $TD_{50}(v_{\text{ref}})$ are the tolerance doses in *Gy* that cause 50 % complication rates within 5 years after treatment for uniform irradiation of the partial volume v according to Eqs. (6.13) and (6.15), and reference volume v_{ref}, respectively. The parameters n and m control the volume effect and the slope of the dose-response curve, respectively. By using an effective volume method (Kutcher and Burman 1989), a nonuniform dose distribution, which has a volume bin v_s with a dose of LQED_s in the differential DVH, was transformed into a uniform dose distribution with an effective volume v_{eff} at the maximum dose of LQED_{max} in Eq. (6.14). The fitting parameter values for the NTCP calculation were obtained from Burman et al. (1991).

6.5.6 Assessment of Usable Beam Arrangements

In practice, treatment planners could manually select the best plan for each patient from among the treatment plans that are based on similar cases, according to the planner's own policies and the patient's performance. However, some indices that are representative of the treatment plan's usefulness could be helpful during decision making. The usefulness of each treatment plan can be estimated by the following Euclidean distance, d_{plan}, of the plan evaluation vector between an ideal treatment plan and each treatment plan that has been determined based on a similar case. This quantity is designated as the RTP evaluation measure:

$$d_{\text{plan}} = \sqrt{\sum_{j=1}^{J} \left(E(\text{ideal})_j - E(\text{plan})_j \right)^2}, \tag{6.16}$$

where J is the number of plan evaluation indices, $E(\text{ideal})_j$ is the j-th plan evaluation index for the ideal treatment plan, and $E(\text{plan})_j$ is the j-th plan evaluation index for the treatment plan based on a similar case. The ideal treatment plan was created under the assumption that it produces perfect, uniform irradiation with a prescription dose in the PTV and no irradiation in the surrounding OARs or normal tissues. Although equal weights for were set for all of the indices in this study, the weights for each index could be determined based on each patient's condition or the treatment planners' policies.

6.5.7 Experimental Results

The proposed method was assessed using an RTP database that included 81 cases of lung cancer (right lung: 46 cases, left lung: 35 cases), as well as 10 test cases (right lung: 3 cases, left lung: 7 cases) that were chosen at random from all 91 available

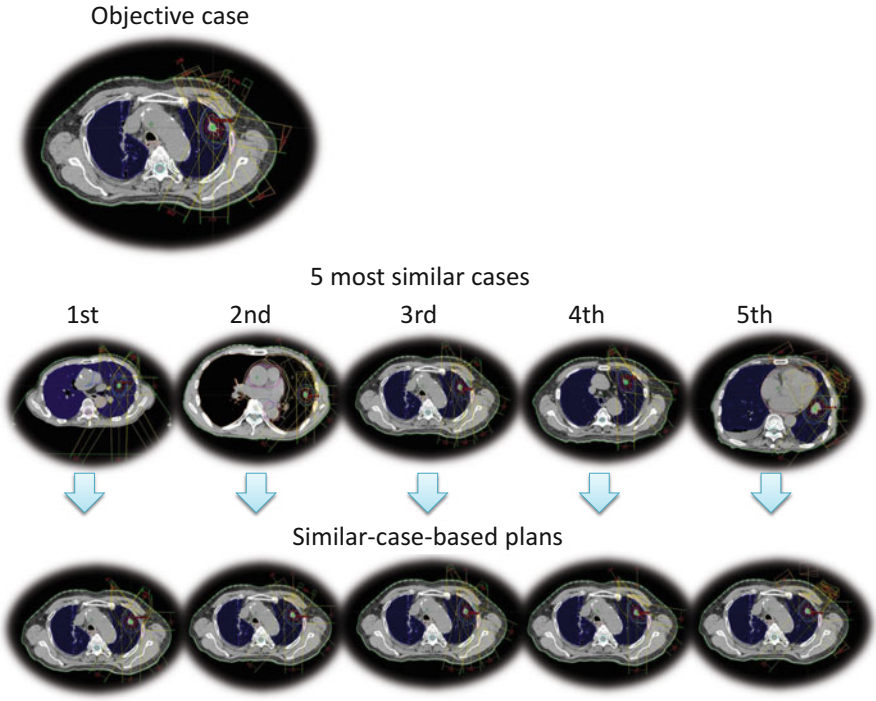

Fig. 6.7 An objective case, the first to fifth most similar cases to the objective case, and similar-case-based treatment plans

cases. The 10 test cases were not included in the RTP database of 81 cases (Magome et al. 2013a, b). The five most similar cases were selected from among the cases of lung cancers that were ipsilateral to the test case. The effectiveness of the combination method of determining the initial beam arrangement based on similar cases and the local optimization of the beam arrangement was evaluated by comparing the planning evaluation indices of 50 plans (5 plans $\times$ 10 test cases) with and without the local optimization of the beam arrangement. The same beam weights and wedges from the similar case were used for the plan, with the beam arrangement determined by our method.

Figure 6.7 shows an objective case, the first to fifth most similar cases to this objective case, and the similar-case-based treatment plans. In practice, a treatment planner could select one of the suitable plans for the patient from among several similar-case-based plans.

Figure 6.8 illustrates dose distributions of the original plan and one of the similar-case-based plan (specifically, the most usable plan). Although the lateral beam passed the spinal cord in the beam arrangement, the optimized beam arrangement avoided the spinal cord. Figure 6.9 provides DVHs for the case shown in Fig. 6.8. Regarding the PTV, the similar-case-based plan had a DVH curve that was almost the same as that of the original plan. However, the similar-case-based plan

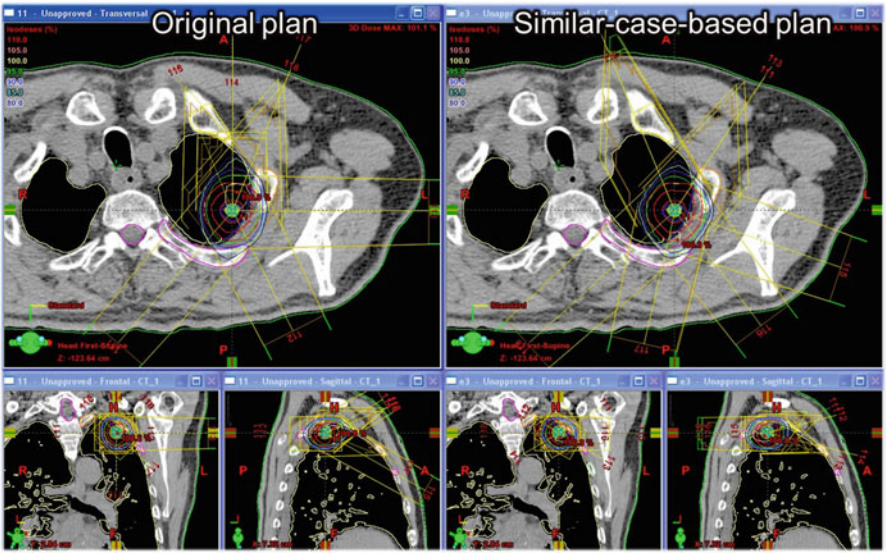

Fig. 6.8 Dose distributions of the original plan and one of the similar-case-based plans

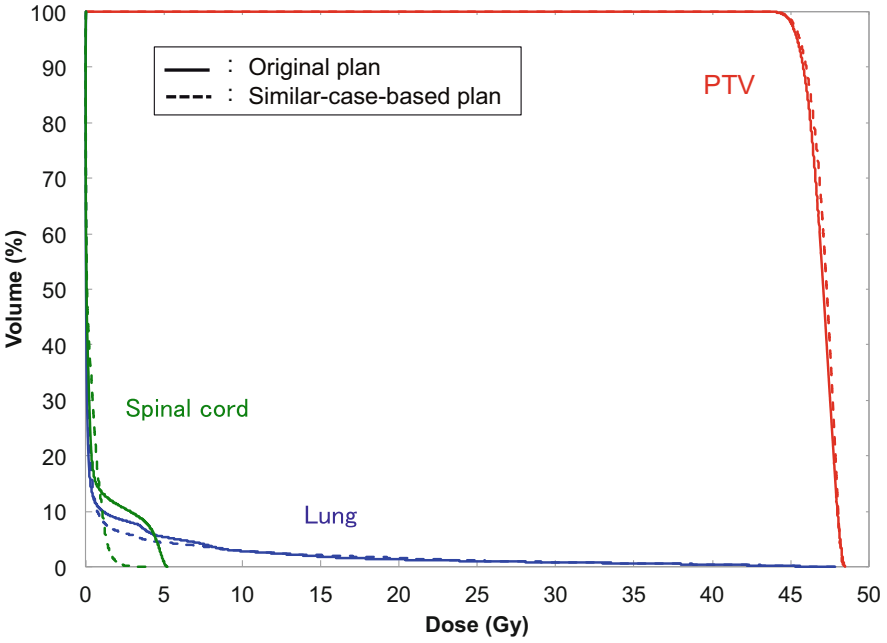

Fig. 6.9 Dose-volume histograms of the original plan and the similar-case-based plan for the case shown in Fig. 6.8

also resulted in better sparing of spinal cord and lung regions, as compared with the original plan. Magome et al. (2013b) have reported detailed results indicating that the local BAO algorithm improved the quality of treatment plans with significant differences ($P < 0.05$) in the homogeneity index and conformity index for the PTV, $V10$, $V20$, mean dose, and NTCP for the lung. Moreover, the proposed method may provide usable beam arrangements that are not significantly different from the original beam arrangements ($P > 0.05$) in terms of the ten planning evaluation indices. The mean value of D95 was significantly improved based on the proposed method, as compared with the D95 of the original beam arrangements ($P = 0.029$).

6.6 Estimation of Available Beam Direction Space

Because collision of the gantry and the patient must be avoided, the available beam direction space is limited by the gantry head, immobilizer, and patient's size. Magome et al. (2013b) constrained the available beam space, and these constraints were used in past cases included in the RTP database. Takayama et al. (2005) determined the applicable areas of beam arrangement at different isocenter heights. Ideally, however, the space should be determined separately for individual patients. Recently, several researchers have developed a collision prediction methodology for the patient and gantry by reconstructing the patient's surface on a treatment couch (Padilla et al. 2015; Yu et al. 2015). These studies allow more extensive use of noncoplanar beam directions, which can provide a better dose distribution.

6.7 Summary and Future Direction

In this chapter, computer-assisted treatment planning approaches for SBRT have been discussed, especially focusing on beam angle optimization and similar-case-based treatment planning. In general, the RTP database at each hospital has been generated by experienced planners after many trials and incorporates substantial amount of their knowledge and skills. The aim of the discussed studies was to use these records of knowledge and skill. The similar-case-based RTP was able to provide several usable beam arrangements based on similar cases in the RTP database. These methods could be useful for treatment planners, thereby improving the quality and efficiency of radiotherapy. Although the plan evaluation indices were calculated to evaluate the treatment plans, they may not cover all aspects of the dose distribution. Regarding the future direction of research, it will be important to incorporate clinical outcomes in order to improve the quality of the RTP database.

Acknowledgments The author would like to thank the radiation oncology group at the University of Tokyo Hospital for their support. This work was supported by a Grant-in-Aid for the Japan Society for the Promotion of Science (JSPS) Fellows (13J02944), as well as by a Grant-in-Aid for Young Scientists (B) (26860397).

References

Aisen AM, Broderick LS, Winer-Muram H, Brodley CE, Kak AC, Pavlopoulou C, Dy J, Shyu CR, Marchiori A (2003) Automated storage and retrieval of thin-section CT images to assist diagnosis: system description and preliminary assessment. Radiology 228(1):265–270

Aleman DM, Kumar A, Ahuja RK, Romeijn HE, Dempsey JF (2008) Neighborhood search approaches to beam orientation optimization in intensity modulated radiation therapy treatment planning. J Glob Optim 42:587–607

Bertsimas D, Cacchiani V, Craft D, Nohadani O (2013) A hybrid approach to beam angle optimization in intensity-modulated radiation therapy. Comput Oper Res 40:2187–2197

Breedveld S, Storchi PRM, Voet PWJ, Heijmen BJM (2012) iCycle: integrated, multicriterial beam angle, and profile optimization for generation of coplanar and noncoplanar IMRT plans. Med Phys 39:951–963

Burger W, Burge MJ (2007) Digital image processing an algorithmic introduction using Java. Springer, New York

Burman C, Kutcher GJ, Emami B, Goitein M (1991) Fitting of normal tissue tolerance data to an analytic function. Int J Radiat Oncol Biol Phys 21:123–135

Chanyavanich V, Das SK, Lee WR, Lo JY (2011) Knowledge-based IMRT treatment planning for prostate cancer. Med Phys 38:2515–2522

Commowick O, Malandain G (2007) Efficient selection of the most similar image in a database for critical structures segmentation. Med Image Comput Comput Assist Interv 10(Pt 2):203–210

de Pooter JA, Romero AM, Jansen WPA, Storchi PRM, Woudstra E, Levendag PC, Heijmen BJM (2006) Computer optimization of noncoplanar beam setups improves stereotactic treatment of liver tumors. Int J Radiat Oncol Biol Phys 66:913–922

de Pooter JA, Romero AM, Wunderink W, Storchi PRM, Heijmen BJM (2008) Automated non-coplanar beam direction optimization improves IMRT in SBRT of liver metastasis. Radiother Oncol 88:376–381

Djajaputra D, Wu Q, Wu Y, Mohan R (2003) Algorithm and performance of a clinical IMRT beam-angle optimization system. Phys Med Biol 48:3191–3212

Gaede S, Wong E, Rasmussen H (2004) An algorithm for systematic selection of beam directions for IMRT. Med Phys 31:376–388

Glide-Hurst CK, Chetty IJ (2014) Improving radiotherapy planning, delivery accuracy, and normal tissue sparing using cutting edge technologies. J Thorac Dis 6:303–318

Holt A, van Vliet-Vroegindeweij C, Mans A, Belderbos JS, Damen EMF (2011) Volumetric-modulated arc therapy for stereotactic body radiation therapy of lung tumors: a comparison with intensity-modulated radiotherapy techniques. Int J Radiat Oncol Biol Phys 81:1560–1567

Hrbacek J, Lang S, Graydon SN, Klöck S, Riesterer O (2014) Dosimetric comparison of flattened and unflattened beams for stereotactic ablative radiotherapy of stage I non-small cell lung cancer. Med Phys 41:031709

ICRU (1999) Prescribing, recording and reporting photon beam therapy (supplement to ICRU report 50). Interna-tional Commission on Radiation Units and Measurements, Bethesda

Kanai T, Matsufuji N, Miyamoto T, Mizoe J, Kamada T, Tsuji H, Kato H, Baba M, Tsujii H (2006) Examination of GyE system for HIMAC carbon therapy. Int J Radiat Oncol Biol Phys 64:650–656

Kumazawa S, Muramatsu C, Li Q, Li F, Shiraishi J, Caligiuri P, Schmidt RA, MacMahon H, Doi K (2008) An investigation of radiologists' perception of lesion similarity: observations with paired breast masses on mammograms and paired lung nodules on CT images. Acad Radiol 15(7):887–894

Kutcher GJ, Burman C (1989) Calculation of complication probability factors for non-uniform normal tissue irradiation: the effective volume method. Int J Radiat Oncol Biol Phys 16:1623–1630

Li Y, Lei J (2010) A feasible solution to the beam-angle-optimization problem in radiotherapy planning with a DNA-based genetic algorithm. IEEE Trans Biomed Eng 57:499–508

Lim DH, Yi BY, Mirmiran A, Dhople A, Suntharalingam M, D'Souza WD (2010) Optimal beam arrangement for stereotactic body radiation therapy delivery in lung tumors. Acta Oncol (Stockh) 49:219–224

Liu R, Buatti JM, Howes TL, Dill J, Modrick JM, Meeks SL (2006) Optimal number of beams for stereotactic body radiation therapy of lung and liver lesions. Int J Radiat Oncol Biol Phys 66:906–912

Lyman JT (1985) Complication probability as assessed from dose-volume histograms. Radiat Res Suppl 8:S13–S19

Magome T, Arimura H, Shioyama Y, Mizoguchi A, Tokunaga C, Nakamura K, Honda H, Ohki M, Toyofuku F, Hirata H (2013a) Computer-aided beam arrangement based on similar cases in radiation treatment-planning databases for stereotactic lung radiation therapy. J Radiat Res 54:569–577

Magome T, Arimura H, Shioyama Y, Nakamura K, Honda H, Hirata H (2013b) Similar-case-based optimization of beam arrangements in stereotactic body radiation therapy for assisting treatment planners. BioMed Res Int 6:1–10

Meyer J, Hummel SM, Cho PS, Austin-Seymour MM, Phillips MH (2005) Automatic selection of non-coplanar beam directions for three-dimensional conformal radiotherapy. Br J Radiol 78:316–327

Mishra N, Petrovic S, Sundar S (2011) A self-adaptive case-based reasoning system for dose planning in prostate cancer radiotherapy. Med Phys 38:6528

Muramatsu C, Li Q, Suzuki K, Schmidt RA, Shiraishi J, Newstead GM, Doi K (2005) Investigation of psychophysical measure for evaluation of similar images for mammographic masses: preliminary results. Med Phys 32(7):2295–2304

Muramatsu C, Li Q, Schmidt RA, Shiraishi J, Doi K (2009) Determination of similarity measures for pairs of mass lesions on mammograms by use of BI-RADS lesion descriptors and image features. Acad Radiol 16(4):443–449

Muramatsu C, Schmidt RA, Shiraishi J, Li Q, Doi K (2010) Presentation of similar images as a reference for distinction between benign and malignant masses on mammograms: analysis of initial observer study. J Digit Imaging 23(5):592–602

Nagata Y, Takayama K, Matsuo Y, Norihisa Y, Mizowaki T, Sakamoto T, Sakamoto M, Mitsumori M, Shibuya K, Araki N, Yano S, Hiraoka M (2005) Clinical outcomes of a phase I/II study of 48 Gy of stereotactic body radiation therapy in 4 fractions for primary lung cancer using a stereotactic body frame. Int J Radiat Oncol Biol Phys 63:1427–1431

Nagata Y, Wulf J, Lax I, Timmerman R, Zimmermann F, Stojkovski I, Jeremic B (2011) Stereotactic Radiotherapy of Primary Lung Cancer and Other Targets: Results of Consultant Meeting of the International Atomic Energy Agency. Int J Radiat Oncol Biol Phys 79:660–669

Nakagawa K, Haga A, Sakumi A, Yamashita H, Igaki H, Shiraki T, Ohtomo K, Iwai Y, Yoda K (2014) Impact of flattening-filter-free techniques on delivery time for lung stereotactic volumetric modulated arc therapy and image quality of concurrent kilovoltage cone-beam computed tomography: a preliminary phantom study. J Radiat Res 55:200–202

Onishi H, Shirato H, Nagata Y, Hiraoka M, Fujino M, Gomi K, Karasawa K, Hayakawa K, Niibe Y, Takai Y, Kimura T, Takeda A, Ouchi A, Hareyama M, Kokubo M, Kozuka T, Arimoto T, Hara R, Itami J, Araki T (2011) Stereotactic body radiotherapy (SBRT) for operable stage I non-small-cell lung cancer: can SBRT be comparable to surgery? Int J Radiat Oncol Biol Phys 81:1352–1358

Padilla L, Pearson EA, Pelizzari CA (2015) Collision prediction software for radiotherapy treatments. Med Phys 42:6448–6456

Potrebko PS, McCurdy BMC, Butler JB, El-Gubtan AS (2008) Improving intensity-modulated radiation therapy using the anatomic beam orientation optimization algorithm. Med Phys 35:2170–2179

Pugachev A, Xing L (2002) Incorporating prior knowledge into beam orientaton optimization in IMRT. Int J Radiat Oncol Biol Phys 54:1565–1574

Rietzel E, Pan T, Chen GTY (2005) Four-dimensional computed tomography: image formation and clinical protocol. Med Phys 32:874–889

Rowbottom CG, Webb S, Oldham M (1999) Beam-orientation customization using an artificial neural network. Phys Med Biol 44:2251

Sanchez-Nieto B, Nahum AE (1999) The delta-TCP concept: A clinically useful measure of tumor control probability. Int J Radiat Oncol Biol Phys 44:369–380

Sanchez-Nieto B, Nahum AE (2000) BIOPLAN: software for the biological evaluation of. Radiotherapy treatment plans. Med Dosim 25:71–76

Schlaefer A, Dieterich S (2011) Feasibility of case-based beam generation for robotic radiosurgery. Artif Intell Med 52:67–75

Shioyama Y, Nakamura K, Sasaki T, Ohga S, Yoshitake T, Nonoshita T, Asai K, Terashima K, Matsumoto K, Hirata H, Honda H (2013) Clinical results of stereotactic body radiotherapy for Stage I small-cell lung cancer: a single institutional experience. J Radiat Res 54:108–112

Takahashi W, Yamashita H, Kida S, Masutani Y, Sakumi A, Ohtomo K, Nakagawa K, Haga A (2013) Verification of Planning Target Volume Settings in Volumetric Modulated Arc Therapy for Stereotactic Body Radiation Therapy by Using In-Treatment 4-Dimensional Cone Beam Computed Tomography. Int J Radiat Oncol Biol Phys 86:426–431

Takayama K, Nagata Y, Negoro Y, Mizowaki T, Sakamoto T, Sakamoto M, Aoki T, Yano S, Koga S, Hiraoka M (2005) Treatment planning of stereotactic radiotherapy for solitary lung tumor. Int J Radiat Oncol Biol Phys 61:1565–1571

Taremi M, Hope A, Dahele M, Pearson S, Fung S, Purdie T, Brade A, Cho J, Sun A, Bissonnette J-P, Bezjak A (2012) Stereotactic Body Radiotherapy for Medically Inoperable Lung Cancer: Prospective, Single-Center Study of 108 Consecutive Patients. Int J Radiat Oncol Biol Phys 82:967–973

Thames HD, Bentzen SM, Turesson I, Overgaard M, Van den Bogaert W (1990) Time-dose factors in radiotherapy: a review of the human data. Radiother Oncol 19:219–235

Timmerman R, Galvin J, Michalski J, Straube W, Ibbott G, Martin E, Abdulrahman R, Swann S, Fowler J, Choy H (2006a) Accreditation and quality assurance for Radiation Therapy Oncology Group: Multicenter clinical trials using Stereotactic Body Radiation Therapy in lung cancer. Acta Oncol (Stockh) 45:779–786

Timmerman R, McGarry R, Yiannoutsos C, Papiez L, Tudor K, DeLuca J, Ewing M, Abdulrahman R, DesRosiers C, Williams M, Fletcher J (2006b) Excessive toxicity when treating central tumors in a phase ii study of stereotactic body radiation therapy for medically inoperable early-stage lung cancer. J Clin Oncol 24:4833–4839

Timmerman RD, Kavanagh BD, Cho LC, Papiez L, Xing L (2007) Stereotactic body radiation therapy in multiple organ sites. J Clin Oncol 25:947–952

Timmerman R, Paulus R, Galvin J, Michalski J, Straube W, Bradley J, Fakiris A, Bezjak A, Videtic G, Johnstone D, Fowler J, Gore E, Choy H (2010) Stereotactic body radiation therapy for inoperable early stage lung cancer. JAMA 303:1070–1076

Underberg RWM, Lagerwaard FJ, Cuijpers JP, Slotman BJ, Van Sörnsen De Koste JR, Senan S (2004) Four-dimensional CT scans for treatment planning in stereotactic radiotherapy for stage I lung cancer. Int J Radiat Oncol Biol Phys 60:1283–1290

Vaitheeswaran R, Narayanan VKS, Bhangle JR, Nirhali A, Kumar N, Basu S, Maiya V (2010) An algorithm for fast beam angle selection in intensity modulated radiotherapy. Med Phys 37:6443–6452

Videtic GMM, Stephans K, Reddy C, Gajdos S, Kolar M, Clouser E, Djemil T (2010) Intensity-modulated radiotherapy-based stereotactic body radiotherapy for medically inoperable early-stage lung cancer: excellent local control. Int J Radiat Oncol Biol Phys 77:344–349

Wang X, Zhang X, Dong L, Liu H, Wu Q, Mohan R (2004) Development of methods for beam angle optimization for IMRT using an accelerated exhaustive search strategy. Int J Radiat Oncol Biol Phys 60:1325–1337

Webb S, Nahum AE (1993) A model for calculating tumour control probability in radiotherapy including the effects of inhomogeneous distributions of dose and clonogenic cell density. Phys Med Biol 38(6):653–666

Wheldon TE, Deehan C, Wheldon EG, Barrett A (1998) The linear-quadratic transformation of dose-volume histograms in fractionated radiotherapy. Radiother Oncol 46:285–295

Yamashita H, Haga A, Takahashi W, Takenaka R, Imae T, Takenaka S, Nakagawa K (2014a) Volumetric modulated arc therapy for lung stereotactic radiation therapy can achieve high local control rates. Radiat Oncol 9:243

Yamashita H, Takahashi W, Haga A, Kida S, Saotome N, Nakagawa K (2014b) Stereotactic body radiotherapy for small lung tumors in the university of Tokyo hospital. BioMed Res Int 2014:1–13

Yu VY, Tran A, Nguyen D, Cao M, Ruan D, Low DA, Sheng K (2015) The development and verification of a highly accurate collision prediction model for automated noncoplanar plan delivery. Med Phys 42:6457–6467

Zhang GG, Ku L, Dilling TJ, Stevens CW, Zhang RR, Li W, Feygelman V (2011) Volumetric modulated arc planning for lung stereotactic body radiotherapy using conventional and unflattened photon beams: a dosimetric comparison with 3D technique. Radiat Oncol (Lond) 6:152